Anal. Bioanal. Electrochem., Vol. 16, No. 9, 2024, 846-861
https://www.doi.org/10.22034/abec.2024.716161

Analytical & Bioanalytical Electrochemistry

Full Paper

Improving The Electrochemical Detection of Profenofos Insecticides Based on Tio$_2$@Nio-Cuo Nanocomposite Doped Graphene Paste Electrode

Muhammad Nurdin,[1,*] Maulidiyah Maulidiyah,[1] Muhammad Zakir Muzakkar,[1] Irwan Irwan,[2] Zul Arham,[3] and Ahmad Zulfan[4]

[1]*Department of Chemistry, Faculty of Mathematics and Natural Sciences, Universitas Halu Oleo, Jl. H.E.A. Mokodompit Kampus Baru Anduonohu, Kendari 93232 – Southeast Sulawesi, Indonesia*
[2]*Department of Pharmacy, Faculty of Sciences and Technology, Institut Teknologi dan Kesehatan Avicenna, Kendari 93117, Southeast Sulawesi, Indonesia*
[3]*Department of Mathematics and Natural Sciences, Institute Agama Islam Negeri (IAIN), Kendari 93563–Southeast Sulawesi, Indonesia*
[4]*Nickel Research Institute, Universitas Muhammadiyah Kendari, Jl. K.H. Ahmad Dahlan, Kendari, Southeast Sulawesi 93117, Indonesia*

*Corresponding Author, Tel.: +6281316551674
E-Mail: mnurdin06@yahoo.com

Received: 23 April 2024 / Received in revised form: 24 September 2024 / Accepted: 28 September 2024 / Published online: 30 September 2024

Abstract- A rapid and facile method for detecting profenofos is crucial for environmental surveillance and ensuring product quality. Electrochemical sensing, as appears presents significant potential as a nascent technology for profenofos detection in recent years. Herein, NiO-CuO bimetallic modified graphene paste electrode/TiO_2 was developed for the detection of profenofos over cyclic voltammetry technique. The TiO_2@NiO-CuO were synthesized through the sol-gel method and characterized by various analyses such as SEM, XRD, and FTIR and electrochemical techniques. The superior electrochemical properties of the suggested GPE/TiO_2@NiO-CuO were demonstrated by cyclic voltammetry investigations performed in $Fe(CN)_6^{4-/3-}$ solution. The electrode performance of GPE/TiO_2 doped with NiO-CuO towards K_3FeCN_6 solution is notably enhanced compared to GPE/TiO_2 undoped. Doping notably increased the conductivity of the GPE/TiO_2, leading to a performance enhancement in the electrocatalytic activity and detection sensitivity of profenofos. Under optimum conditions, the GPE/TiO_2@NiO-CuO demonstrated an impressively low detection limit of 0.00132 µg/L, coupled with a favorable detection range spanning from 1.0 µg/L to 10 µg/L with correlation coefficient R^2 = 0.992. Moreover, the electrode demonstrates remarkably very good stability,

and repeatability with %RSD is only 0.94% over 11 repeated measurements. These results signify that GPE/TiO_2@NiO-CuO for detecting profenofos, demonstrates exceptional excellent linearity, repeatability, and promising sensitivity for pesticide detection.

Keywords- GPE/TiO_2; NiO-CuO nanocomposite; Electrochemical detection; Cyclic voltammetry; Profenofos insecticide

1. INTRODUCTION

In the era of globalization, the preservation and protection of food, particularly against the potential contamination of various chemical substances, have become a central issue in various countries [1]. As a strategic effort to ensure food security, humans have created chemical pesticides as early protection agents to safeguard crops from pest attacks and other diseases. Generally, the use of pesticides in agriculture can assist farmers in achieving higher yields. Additionally, other benefits include increased crop productivity, protection against crop damage from weed/pest infestations, disease control, and improved food quality. On one hand, the disproportionate use of pesticides in terms of type, target, and dosage can have environmental repercussions, leading to contamination [2,3].

Various types of pesticides have been widely reported, such as organophosphates, organochlorines, pyrethroids, and carbamates. In practice, the most extensively used pesticides in the field belong to the organophosphate group, with profenofos being a notable example [4]. The molecular structure of profenofos comprises a heterocyclic ring containing a phosphorus atom bound to three alkyl groups, along with an oxygen and sulfur group attached to phosphorus. Despite its effectiveness in controlling pests, the use of profenofos also poses potential risks to human health [5,6]. Long-term exposure to profenofos can result in serious health risks, including neurological disorders, nerve damage, and respiratory issues [7]. Additionally, some compounds within the organophosphate group can easily transfer from breastfeeding mothers to infants through breast milk [8]. Consequently, their presence is identified as a major source of pollution concerning food safety and human health protection [9].

In recent years, various methods have been reported in the literature for the detection of profenofos pesticides, such as gas chromatography [10], fluorescence spectrophotometry [11], high-performance liquid chromatography [12], and electrochemistry [4,13]. However, the development of electrochemical methods has garnered significant attention among researchers. Unlike spectroscopy and chromatography methods, electrode-modified electrochemical methods offer an ultra-sensitive, portable, stable, rapidly measurable, cost-effective, and easily applicable system [14]. Electrochemical methods based on modified electrodes fundamentally operate on the principle of voltammetry. The advantages of this technique include high sensitivity, low detection limits, low analysis costs, and fast analysis times [15–17]. In its application, this technique requires three electrodes: a reference electrode, an auxiliary

electrode, and a working electrode [18–20]. To date, most electrochemical sensors have been modified with the use of nano-metal materials, providing various special functions such as catalytic properties and high conductivity.

Among nano materials, titanium dioxide nanoparticles (TiO_2) have garnered significant attention due to their unique properties such as high conductivity, non-toxicity, and environmental friendliness [21–24]. However, it appears that TiO2 still has limitations in its electrical properties, including limited ionic diffusivity, low electrode conductivity, and high resistance at the electrode-electrolyte interface in solutions [25–27]. To overcome these limitations, several important strategies have been employed to enhance the electrochemical properties of TiO_2. Recently, numerous studies have indicated that combining TiO_2 with bimetallic catalysts such as NiO and CuO can improve the electrochemical activity of the electrode. This is based on the semiconductor's photocatalytic ability, enhanced thermal stability, and control over the electrode surface morphology. Based on previous reports, bimetallic and multivalent catalysts have proven to exhibit high stability, chemical activity, and excellent durability [28–30]. Additionally, the NiO-CuO alloy provides more active sites for analyte detection, thereby enhancing detection sensitivity. However, more attention needs to be given to developing NiO-CuO alloys for profenofos detection.

In this research, as part of our efforts, we have studied electrode substrates to enhance the performance and stability of the active material. Among the reported electrode substrates, carbon-based materials such as graphene have garnered more attention due to their high conductivity, remarkable mechanical properties, and large surface area. Electrochemical sensors based on graphene-modified TiO_2 electrodes have been previously reported in our research. Although the GPE/TiO_2 electrode exhibits excellent performance, its sensitivity is still significantly limited. Therefore, based on the advantages of combining TiO_2 with bimetallic catalysts such as NiO-CuO mentioned above (GPE/TiO_2@NiO-CuO), it is a very suitable choice for the detection of the pesticide profenofos in the environment.

2. EXPERIMENTAL SECTION

2.1. Chemicals and instruments

All reagents used in this study were employed without further purification. Graphene powder, titanium tetraisopropoxide (TTIP), ethanol (C_2H_5OH), acetic acid (CH_3COOH), acetylacetone, $NiSO_4$ powder, $CuSO_4$ powder, nitric acid, potassium ferrocyanide, and standard profenofos were purchased from Sigma-Aldrich. Additionally, electrochemical measurements such as cyclic voltammetry (CV) were conducted using the Gamry 600 Potentiostat system. Original graphene paste working electrodes (GPE) or modified GPE (4mm diameter), Ag/AgCl reference electrode, and platinum wire were respectively utilized as the working, reference, and counter electrodes.The crystal structure of the electrode materials was analyzed by X-ray diffraction (XRD). Infrared spectra were recorded using a Spectrum One

FT-IR spectrometer in the range of 4000 to 400 cm^{-1}. Furthermore, the surface morphology of the electrode materials was characterized using scanning electron microscopy (SEM).

2.2. Synthesis of TiO_2@NiO-CuO nanocomposite

The TiO_2@NiO-CuO nanocomposite was synthesized through the hydrolysis of titanium tetraisopropoxide (TTIP) with slight modifications from our previous research [31]. In brief, 4.0 mL of TTIP, 15 mL of ethanol, and 0.5 mL of acetylacetone were reacted with 15 mL of ethanol, 1.0 mL of acetic acid, and 2.0 mL of distilled water. The solution mixture was then refluxed for 3 h at 50 °C while continuously stirred using a magnetic stirrer. Subsequently, 1.0 mL of $NiSO_4$ was added as the NiO source, and 1.0 mL of $CuSO_4$ was added as the CuO source until a gel was formed. After the reflux process was completed, the formed gel was evaporated at room temperature for 48 hours until no liquid remained. The subsequent step involved calcination at 400 °C for 1 hour to produce the TiO_2@NiO-CuO nanocomposite.

2.3. Preparation of TiO_2@NiO-CuO working electrode

The TiO_2@NiO-CuO electrode was prepared by weighing 0.7 g of graphene into a watch glass. Subsequently, 0.3 g of paraffin oil and 0.1 g of the TiO_2@NiO-CuO nanocomposite were added to the graphene in the watch glass. The paraffin oil was then heated to a temperature of 80°C. Mechanical stirring was employed to ensure the thorough homogenization of the electrode composite. The homogenized composite was then placed into a tubular-shaped electrode body (ϕ = ±4.0 mm) and connected to a copper wire. The schematic representation of the electrode body containing GPE/TiO_2@NiO-CuO is illustrated in Figure 1.

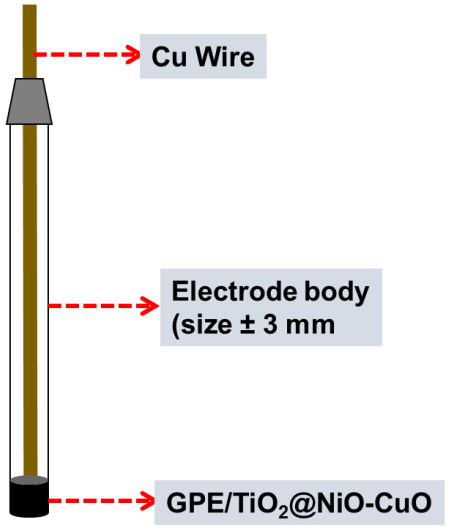

Figure 1. Illustration of the working electrode body

2.4. Electrochemical measurements

The working electrodes (GPE/TiO_2@NiO-CuO and GPE/TiO_2) were investigated using the cyclic voltammetry technique. Voltammograms were recorded in a potential range of −0.8 to 0.8 V with a scan rate of 100 mV s^{-1}. Initially, the electrodes were tested in a 0.01 M electrolyte solution of $[Fe(CN)_6]^{3-/4-}$ to observe the redox peak currents of the fabricated electrodes. Subsequently, the GPE/TiO_2@NiO-CuO electrode was examined in a standard solution of profenofos at a concentration of 10 µg/L, which was prepared in 0.1 M $NaNO_3$. The schematic experimental design of profenofos detection by CV can be seen in Figure 2.

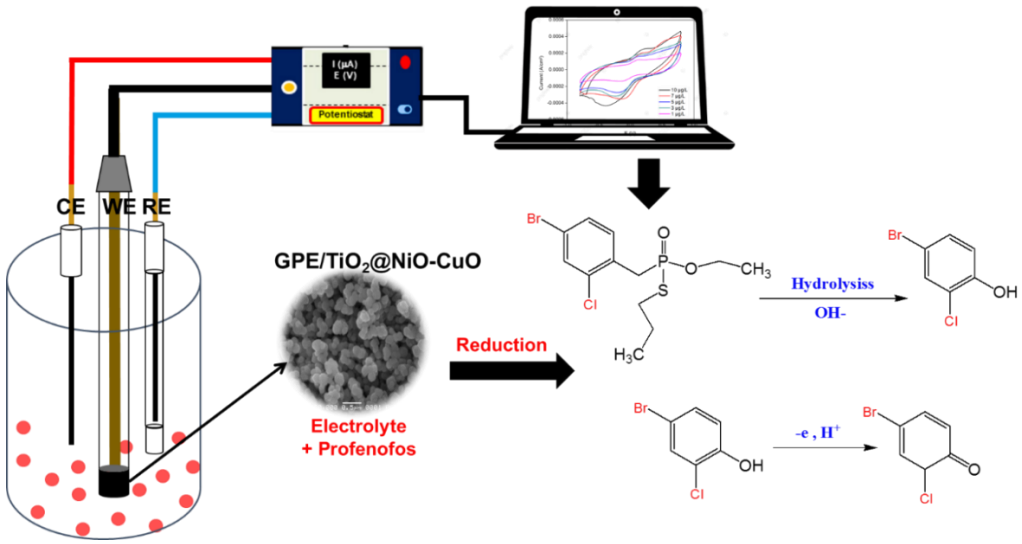

Figure 2. Experimental design of profenofos detection by CV

3. RESULTS AND DISCUSSION

3.1. SEM-EDX Analysis

Based on Figure 3, at a glance, the morphological characteristics of the GPE/TiO_2@NiO-CuO electrode and the undoped GPE/TiO_2 electrode appear almost identical, both exhibiting a spherical shape. However, upon closer inspection, there are notable morphological differences between the two electrodes. The undoped GPE/TiO_2 electrode (Figure 2a) reveals larger and non-uniformly sized TiO_2 particles. These TiO_2 particles tend to aggregate, resulting in insufficient interparticle spacing and a reduced active electrode surface area [32]. In contrast, the GPE/TiO_2@NiO-CuO electrode (Figure 2b) exhibits a more uniform distribution of TiO_2 particles with enhanced interparticle spacing, contributing to a larger active electrode surface area. Additionally, the incorporation of NiO-CuO enhances the porosity of the electrode, as evidenced by the formation of pores around the TiO_2 particles [33,34]. The improved homogeneity and porosity of the GPE/TiO_2@NiO-CuO electrode lead to increased catalytic activity. This is attributed to the larger active surface area of the electrode, which enhances its

capability for catalyzing reactions. Overall, the addition of NiO-CuO doping enhances the morphology of the GPE/TiO_2 electrode, consequently impacting the catalytic activity of the electrode in the detection of the analyte.

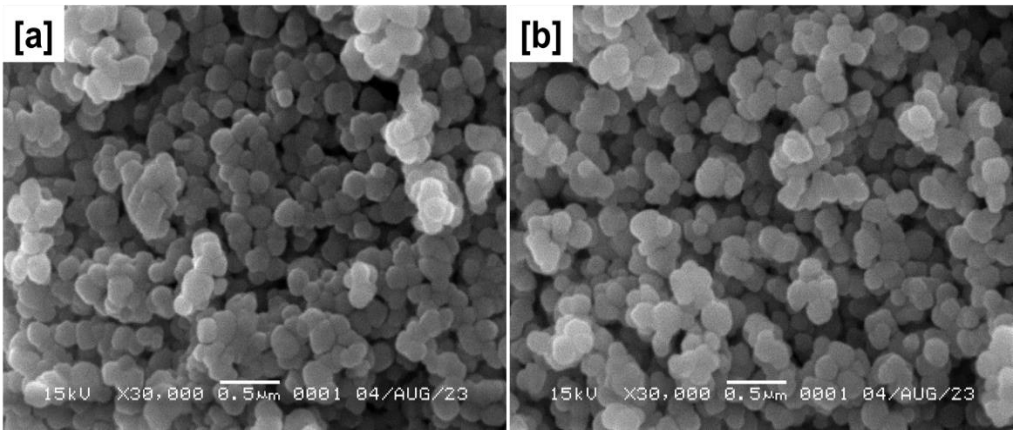

Figure 3. Results of morphological analysis over synthesized nanocomposite; (a) $NpTiO_2$ and (b) TiO_2@NiO-CuO

3.2. XRD Analysis

In this study, the TiO_2@NiO-CuO nanocomposite was successfully synthesized using the sol-gel method. Before electrode preparation, we conducted XRD analysis on the $NpTiO_2$ sample and the TiO_2@NiO-CuO nanocomposite. The analysis results revealed that the XRD spectrum of the $NpTiO_2$ (black curve) sample exhibited at least three specific peaks at angles $2\theta = 25°$, 36°, and 48° [35]. These peaks corresponded to the standard diffraction peaks for TiO_2 anatase (JCPDS file no. 21-1272) and could be associated with the Bragg planes (101), (004), and (110) [19]. As shown in the figure, the X-ray diffraction pattern of the TiO_2@NiO-CuO (red curve) nanocomposite displayed peaks that were nearly identical to those of the $NpTiO_2$ diffraction pattern. However, some differences were observed, including changes in the intensity of diffraction peaks in the TiO_2@NiO-CuO nanocomposite. This can be attributed to the presence of Ni and Cu atoms embedded in the crystal lattice of $NpTiO_2$. The smaller sizes of Ni and Cu atoms compared to Ti atoms can induce lattice disruptions, indicating that NiO and CuO enhance the active surface area of TiO_2. Additionally, there were alterations in the positions of the diffraction peaks in the TiO_2@NiO-CuO nanocomposite compared to the $NpTiO_2$ diffraction peaks. This shift is attributed to the interactions between Ni and Cu atoms with Ti atoms. The presence of NiO and CuO induces slight shifts in the diffraction peak positions, signifying the formation of new crystal structures or modifications in the existing crystal lattice due to the interactions between these elements.

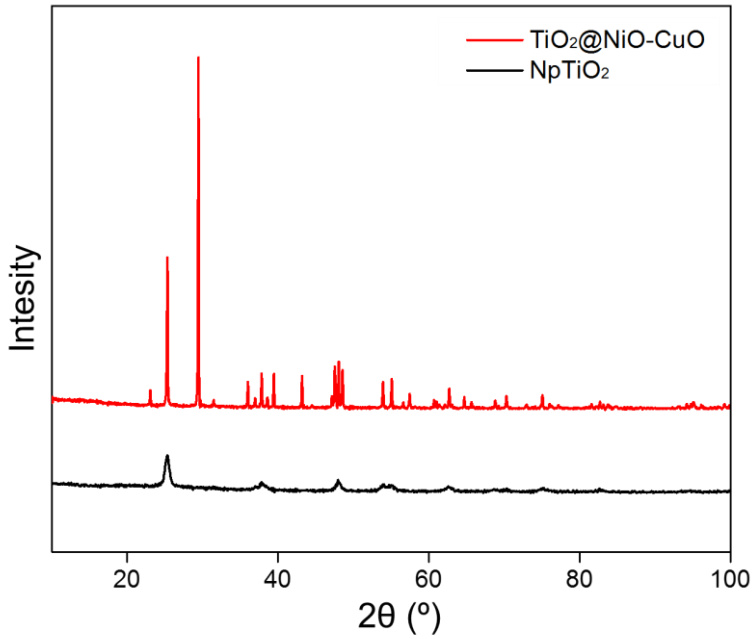

Figure 4. XRD pattern of $NpTiO_2$ (blck curve) and TiO_2@NiO-CuO nanocomposite (red curve)

3.3. FTIR Analysis

The results of the FTIR analysis for $NpTiO_2$ and the TiO_2@NiO-CuO composite are presented in Figure 5. FTIR analysis was conducted to investigate the structural and chemical changes in $NpTiO_2$ and the TiO_2@NiO-CuO composite. In the FTIR spectrum of $NpTiO_2$, several significant peaks are observed, as depicted in Figure 5a. Based on Figure 4a, peaks in the range of 400-700 cm^{-1} are associated with the Ti-O-Ti vibrational modes in the crystal structure of TiO_2, while peaks around 1400-1600 cm^{-1} represent the O-H bond vibrations from adsorbed water on the nanoparticle surface. Furthermore, in the FTIR spectrum of the TiO_2@NiO-CuO composite (Figure 5b), there are shifts and increased intensities in some peaks, indicating modifications in the TiO_2 structure. Peaks in the range of 400-700 cm^{-1} may suggest interactions between TiO_2 and NiO-CuO, possibly involving new chemical bonds or changes in the crystalline state of TiO_2 [36]. Additionally, peaks at 1400-1600 cm^{-1} provide information about changes in O-H bonds and the potential presence of new functional groups due to the modification [37]. Moreover, the possibility of new peaks in this spectrum may reflect interactions between NiO-CuO and TiO_2. A new absorption band appears at the wavenumber of 550 cm^{-1}, resulting from the Ni-O-Ti bond vibration. This absorption band indicates the interaction between Ni and Ti atoms in the TiO_2 crystal lattice [38] . Based on these observations, the addition of NiO and CuO could lead to the growth of TiO_2 particles, rendering them smaller and more homogeneous. Smaller TiO_2 particles exhibit lower absorption band intensities.

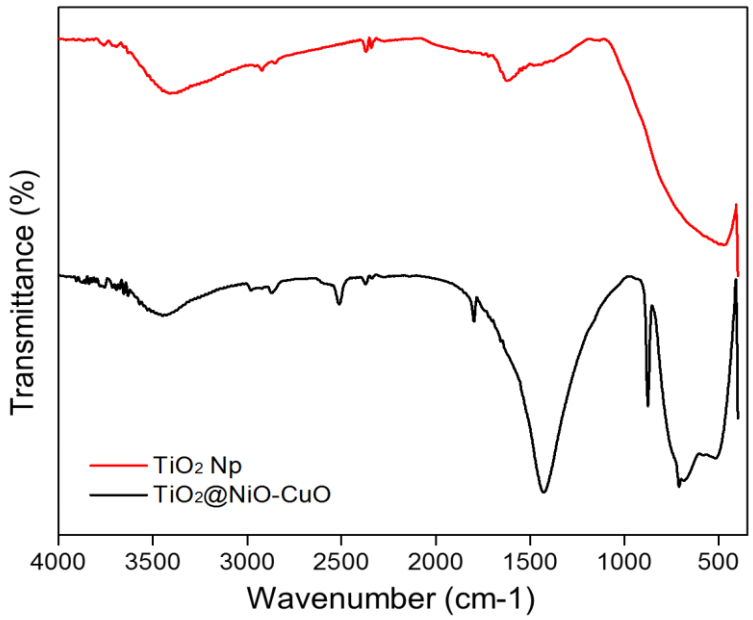

Figure 5. FTIR spectra of NpTiO$_2$ (red curve) and TiO$_2$@NiO-CuO nanocomposites (black curve)

3.4. Electrode performance test in K$_3$[Fe(CN)$_6$] solution

The performance of GPE/TiO$_2$ and GPE/TiO$_2$@NiO-CuO in the K$_3$[Fe(CN)$_6$] system was investigated through various electrochemical parameters, as displayed in Figure 6. Cyclic voltammetry (CV) measurements were conducted within a potential range of -0.8 to 0.8 V at a scan rate of 0.1 V/s [39]. The CV results revealed distinct electrochemical behaviors for the two electrodes. In Figure 6a, the GPE/TiO$_2$ (black curve) exhibited relatively lower peak currents and broader peak separation compared to the GPE/TiO$_2$@NiO-CuO (red curve). This indicates that the incorporation of NiO-CuO onto the TiO$_2$ electrode enhances the electrochemical activity and facilitates faster electron transfer kinetics. Furthermore, GPE/TiO$_2$@NiO-CuO demonstrated a more stable current response compared to the GPE/TiO$_2$. This sustained electrocatalytic activity can be attributed to the catalytic properties of NiO-CuO, contributing to the oxidation-reduction reactions of K$_3$[Fe(CN)$_6$] and facilitating efficient electron transfer processes.

Moreover, to further investigate the effect of NiO-CuO in the GPE/TiO$_2$ electrode, a variation in the mass modifier was carried out. The masses of NiO-CuO used were (0 g, 0.1 g, 0.2 g, and 0.3 g) (Figure 6b). It is observed that the cyclic voltammetry (CV) profiles of the three different masses of NiO-CuO exhibit characteristic redox peaks corresponding to the $Fe(CN)_6^{3-}/Fe(CN)_6^{4-}$ redox couple, indicating good electrochemical behavior. The redox peak currents show a significant enhancement with increasing NiO-CuO content, suggesting improved electron transfer kinetics. The observed enhancement in electrochemical performance can be attributed to the synergistic effect of NiO and CuO, acting as efficient

electron carriers and providing additional active sites for redox reactions. The optimal mass of NiO-CuO is found to be 0.2 g, where the electrode demonstrates the best electrochemical performance with improved charge transfer kinetics and high redox peak currents.

The performance of the GPE/TiO_2@NiO-CuO electrode was also further evaluated by varying the scan rate (2 V/s, 0.1 V/s, 0.05 V/s, and 0.02 V/s) in a $K_3[Fe(CN)_6]$ electrolyte solution. Four different scan rates were employed to explore their influence on the electrochemical behavior of the electrode. The results revealed distinct trends in the electrochemical response with changes in the scan rate (Figure 6c,d). It is evident that at a scan rate of 0.2 V/s, the electrochemical process exhibited a higher current response, indicating a faster charge transfer rate. This observation can be associated with an enhanced redox reaction kinetics facilitated by the higher scan rate [40]. However, as the scan rate decreased to 0.1 V/s, 0.05 V/s, and 0.02 V/s, a gradual decrease in peak current occurred, indicating a reduction in the charge transfer rate. Conversely, lower scan rates resulted in a gradual reduction in peak current, suggesting a slower charge transfer rate.

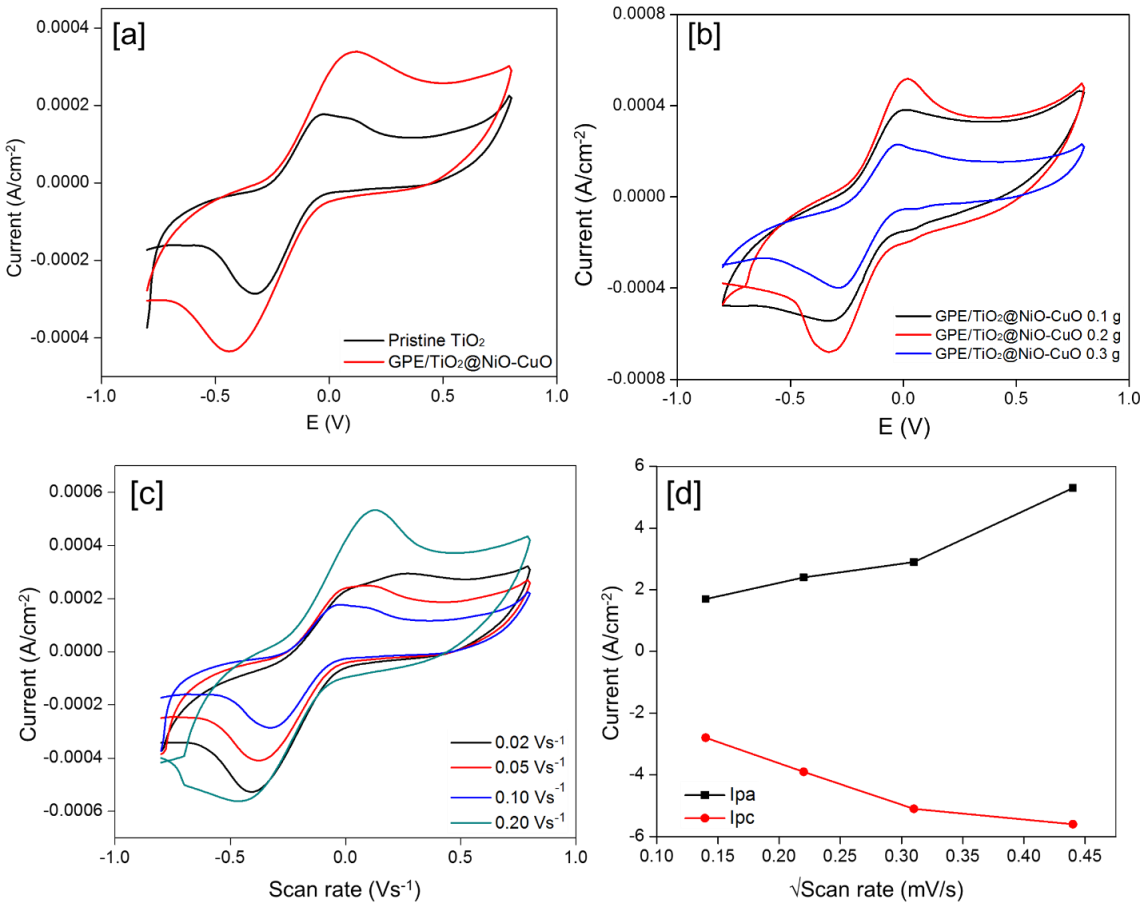

Figure 6. The CV graph by comparing working electrodes in $K_3[Fe(CN)_6]$ as an electrolyte solution (b) CV of GPE/TiO_2@NiO-CuO nanocomposite with the mass variation of NiO-CuO; (c) Effect of scan rate variations on K_3FeCN_6 peak current and [d] Plot of root scan rate vs peak current

3.5. Performance test of GPE/TiO_2@NiO-CuO in profenofos detection

3.5.1. Effect of scan rate variations

In the detection of profenofos, the scan rate plays a crucial role in controlling the electrochemical reaction rate and influencing the electrode response to the target compound. The variation in scan rates employed in this study includes 0.2 V/s, 0.1 V/s, 0.05 V/s, and 0.02 V/s (Figure 7). It is evident that a significant correlation exists between the scan rate and the response of the GPE/TiO_2@NiO-CuO electrode. At a scan rate of 0.2 V/s, there is an observable increase in the electrode current response corresponding to the higher scanning speed [41]. This phenomenon can be attributed to the accelerated electrochemical charge transfer, resulting in a faster current response to profenofos. Conversely, at the lower scan rate of 0.02 V/s, the GPE/TiO_2@NiO-CuO electrode exhibits a noticeable decrease in current. This decline can be explained by the limited time provided for the electrode to respond to profenofos, leading to a lower current response. Higher scan rates enhance the electrode's sensitivity by facilitating quicker charge transfer, while lower scan rates may result in reduced sensitivity due to the restricted response time.

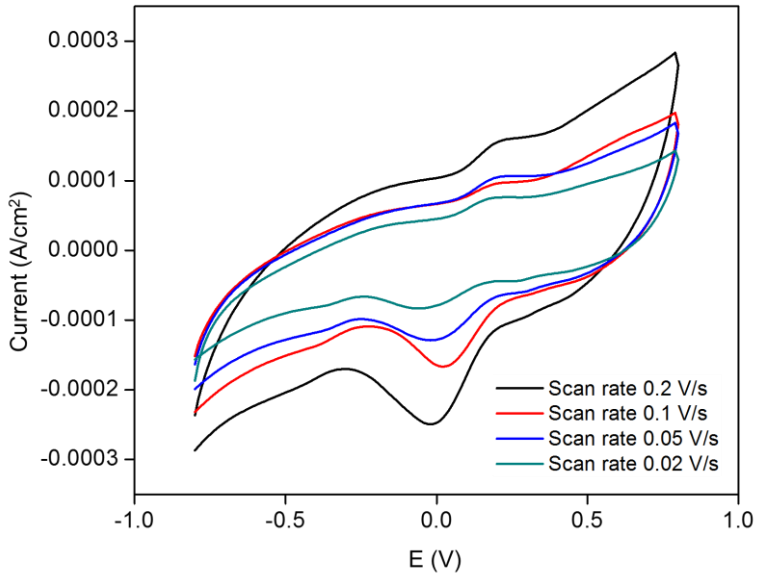

Figure 7. CV of profenofos reduction over GPE/TiO_2@NiO-CuO under a different scan rate

3.5.2. Effect of pH variations

The performance of the GPE/TiO_2@NiO-CuO electrode in detecting profenofos was evaluated under varying pH conditions (3, 4, 5, 6, 7, and 8). pH is a critical factor influencing the electrochemical behavior and efficiency of the electrode in detecting the analyte. In this study, we observed distinct changes in the electrochemical response as a function of pH. Measurement results indicated that pH variations significantly affected the electrode's response to profenofos (Figure 8). It was evident that in the pH range of 3 to 6, the electrochemical

detection of profenofos exhibited increased sensitivity. This phenomenon can be attributed to the enhanced availability of electroactive species and improved electron transfer kinetics under acidic conditions. The acidic environment likely facilitated the protonation of functional groups on the electrode's surface, thereby enhancing the adsorption of profenofos and promoting the electrochemical reactions involved in its detection.

Interestingly, at pH 6, the electrode response demonstrates its optimal performance in detecting profenofos. This pH value can be considered as the optimum condition for the GPE/TiO_2@NiO-CuO in detecting profenofos. This phenomenon can be attributed to the balanced interaction between active sites on the electrode surface and the ionization state of profenofos, thereby resulting in enhanced detection capabilities. Conversely, as the pH increases (to 7 and 8), there is a decline in the electrochemical response. This may be attributed to the deprotonation of specific functional groups on the electrode surface, leading to an overall decrease in sensitivity. Thus, the electrode performance appears to be dependent on pH, with pH 6 identified as the optimal condition for profenofos detection.

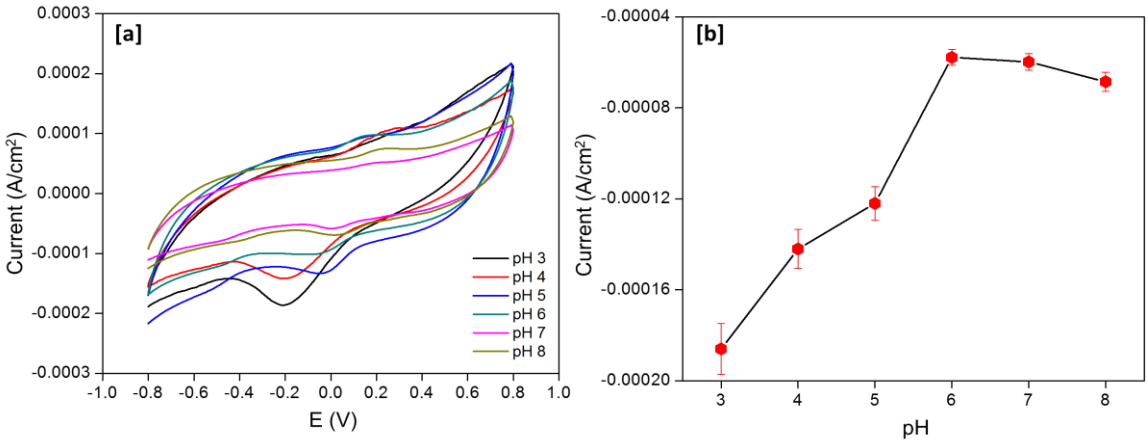

Figure 8. (a) CV of profenofos containing the HCl + citric buffer with pH variation, and (b) Curve between current (Ipc) peaks versus pH

3.5.3. Limit of detection test

The performance of the GPE/TiO_2@NiO-CuO in detecting the pesticide profenofos was systematically evaluated across various concentrations, namely 1 ppm, 3 ppm, 5 ppm, 7 ppm, and 10 ppm. The electrochemical response exhibited a concentration-dependent trend, enabling the determination of the limit of detection (LOD) for profenofos detection (Figure 9). It was observed that as the concentration of profenofos increased from 1 ppm to 10 ppm, there was an increase in the current response. The electrode demonstrated a linear correlation between the concentration of profenofos and the peak current, indicating its good detection capability within the tested range [42]. At a concentration of 1 ppm, a clear current response was observed, demonstrating the electrode's ability to detect profenofos at relatively low

concentrations. As the concentration increased up to 10 ppm, the electrochemical signal also increased proportionally, indicating the electrode's sensitivity to changes in profenofos concentration. Based on the obtained limit of detection (LOD) measurement of 0.00132 µg/L, it shows the remarkable sensitivity of the GPE/TiO_2@NiO-CuO in detecting low concentrations of profenofos.

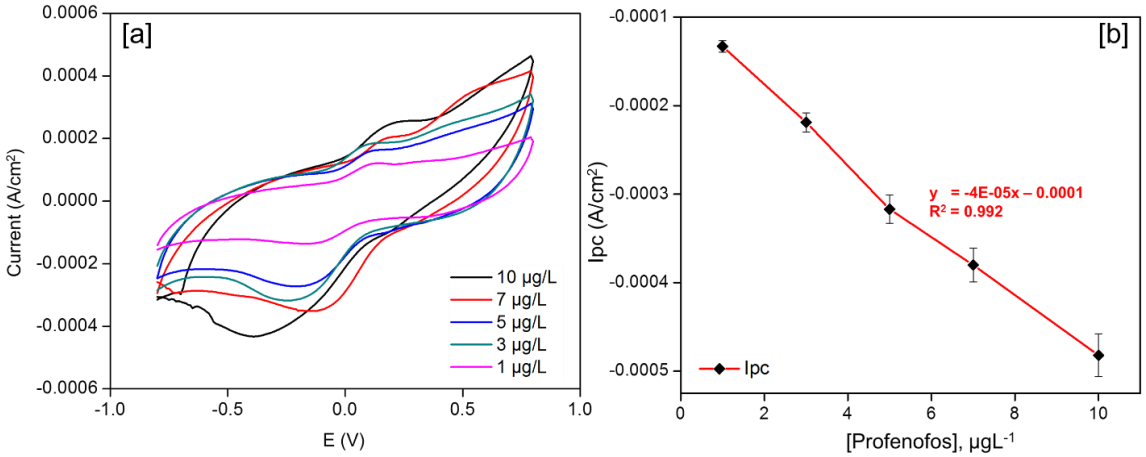

Figure 9. Cyclic voltammograms of profenofos with various concentrations (1 μgL^{-1} – 10 μgL^{-1}) and (b) linear concentration graph of profenofos based on Ipc value

3.5.4. Interfering compounds test and repeatability

Moreover, in this study, the influence of an interfering compound (fipronil) on the detection of profenofos was also investigated. As displayed in Figure 10, the presence of fipronil was observed to affect the detection of profenofos. Cyclic voltammetry analysis revealed changes in the current, which could be directly attributed to the presence of fipronil.

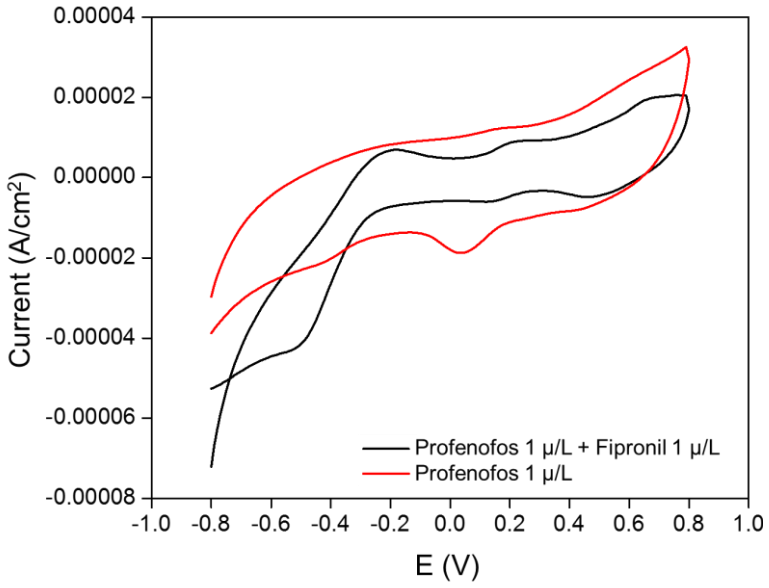

Figure 10. Effect interfering compound on the peak current of profenofos

The presence of fipronil exerted an influence on the current and potential of the electrode. This phenomenon is likely attributed to surface modifications of the electrode and alterations in its conductive or capacitive characteristics. Additionally, the formation of complexes between fipronil and electrode components may lead to the observed current response. Nevertheless, despite the interference of the interfering compound, GPE/TiO_2@NiO-CuO maintained its ability to detect profenofos with high precision.

The electrode repeatability test in detecting profenofos was conducted with 11 repetitions. As depicted in Figure 11, the electrode exhibited consistent and significant current responses. With each of the 11 repeated measurements, the calculation of the Relative Standard Deviation (%RSD) of the electrode's response to profenofos provided an insight into the level of stability and consistency of the results. A low %RSD value indicates that the GPE/TiO_2@NiO-CuO electrode yields relatively uniform responses in each measurement. In other words, the variation among the measurement results is relatively small, supporting the electrode's reliability in consistently detecting profenofos. Based on the measurement results, the %RSD value obtained was 0.94%.

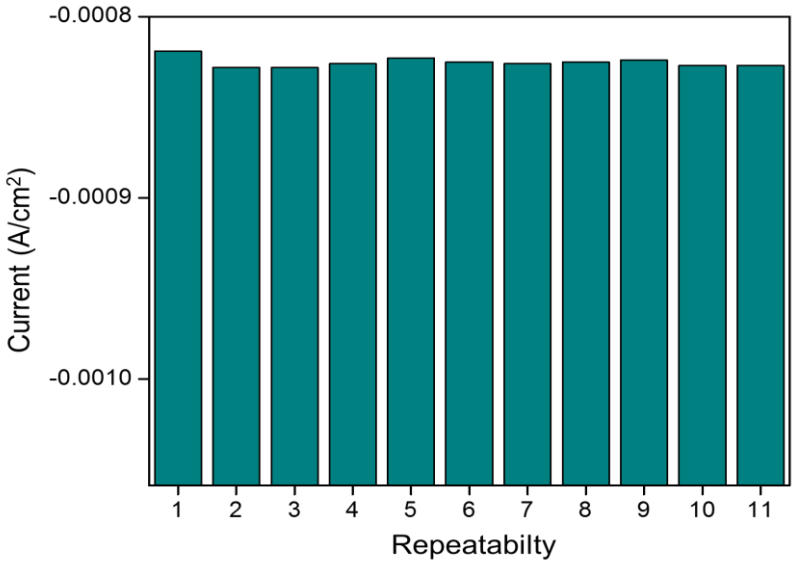

Figure 11. Histogram of repeatability detection of profenofos

Table 1. Comparison of previous detection results for profenofos based on voltammetry

Electrode	**Modifier**	**Method**	**LOD (µg/L)**	**Reference**
GCE	3D-CNTs@MIP	CV	0.002	[43]
CPE	TiO_2	CV	4.0 × 10–5	[4]
MWCNTs	Au@AgNPs	CV	0.0532	[44]
GPE/TiO_2	NiO-CuO composite	CV	0.00132	**This work**

4. CONCLUSION

In this work, we have developed an approach electrochemical for the rapid detection of profenofos over the NiO-CuO bimetallic modified graphene paste electrode/TiO_2. The GPE/TiO_2@NiO-CuO have been successfully prepared via simple sol-gel methods. The characteristics of the electrochemical behavior of the GPE/TiO_2@NiO-CuO were successfully performed using the cyclic voltammetry technique. The electrode's impressive characteristics, including its wide linear range, low detection limit, and high sensitivity, are primarily attributed to the combined effects of graphene's efficient electron transfer, the large surface area of TiO_2, and the effect synergic from NiO-CuO bimetallic. The existence of NiO-CuO bimetallic enhances the sensing current of profenofos. Based on this, we are confident the utilization of an electrochemically modified electrode incorporating a nanocomposite of GPE/TiO_2@NiO-CuO demonstrates promising prospects for the detection of pesticides within the environmental field and plant protection.

Funding

This study was financially supported by the National Research and Innovation Agency (BRIN) with the scheme Innovation for Advanced Indonesia (RIIM) Funding No. 32/IV/KS/05/2023 and 1026/UN29.20/KS/2023 by Indonesian Endowment Funds for Education (LPDP), The Ministry of Finance, Republic of Indonesia. The authors express their gratitude to the Titani Riset Group for the facilities and characterization.

Declarations of interest

The authors declare no conflict of interest in this reported work.

REFERENCES

[1] D.T. Armanda, J.B. Guinée, and A. Tukker, Food Sec. 22 (2019) 13.
[2] K.S. Rajmohan, R. Chandrasekaran, and S. Varjani, Indian J. Microbiol. 60 (2020) 125.
[3] C. Román, J. Llorens, A. Uribeetxebarria, R. Sanz, S. Planas, and J. Arnó, Biosyst. Eng. 195 (2020) 42.
[4] T. Azis, M. Maulidiyah, M.Z. Muzakkar, R. Ratna, S.W. Aziza, C.M. Bijang, O.A. Prabowo, D. Wibowo, and M. Nurdin, Surf. Eng. Appl. Electrochem. 57 (2021) 387.
[5] M. Al-Emran, N.A. Hasan, M.P. Khan, S.M.M. Islam, A. Bashar, I. Zulfahmi, M. Shahjahan, and K.A. Sumon, Environ. Sci. Pollut. Res. (2022) 1.
[6] P.R.S. Soares, W.G. Birolli, I.M. Ferreira, and A.L.M. Porto, Mar. Pollut. Bull. 166 (2021) 112185.
[7] A. Chatterjee, R. Bhattacharya, S. Chatterjee, and N.C. Saha, Comp. Biochem. Physiol. Part C Toxicol. Pharmacol. 242 (2021) 108943.

[8] G. Zheng, E. Schreder, J.C. Dempsey, N. Uding, V. Chu, G. Andres, S. Sathyanarayana, and A. Salamova, Environ. Sci. Technol. Lett. 8 (2021) 224.
[9] V. Terziev, and S. Petkova-Georgieva, IJASOS-International E-Journal Adv. Soc. Sci. 5 (2019).
[10] A.A. Wani, A.A. Dar, I. Jan, M. Mukhtar, K.A. Sofi, G.I. Hassan, and J.A. Sofi, Biomed. Chromatogr. 36 (2022) e5335.
[11] Y. Cai, J. Fang, B. Wang, F. Zhang, G. Shao, and Y. Liu, Sens. Actuators B Chem. 292 (2019) 156.
[12] U.D. Pawar, C.D. Pawar, U.K. Kulkarni, and R.K. Pardeshi, JPC–Journal Planar Chromatogr. TLC 33 (2020) 203.
[13] N. Nesakumar, I. Suresh, G.B. Jegadeesan, J.B.B. Rayappan, and A.J. Kulandaiswamy, Measurement 202 (2022) 111807.
[14] A.B. Kanu, J. Chromatogr. A 1654 (2021) 462444.
[15] M. Nurdin, N. Dali, I. Irwan, M. Maulidiyah, Z. Arham, R. Ruslan, B. Hamzah, S. Sarjuna, and D. Wibowo, Anal. Bioanal. Electrochem. 10 (2018) 1538.
[16] M. Nurdin, M.Z. Muzakkar, M. Maulidiyah, C. Sumarni, T. Azis, R. Ratna, M. Natsir, I. Irwan, L.O.A. Salim, and A.A. Umar, J. Appl. Electrochem. (2022) 1.
[17] M. Nurdin, I. Ilham, M. Maulidiyah, M.Z. Muzakkar, D. Wibowo, Z. Arham, L.O.A. Salim, I. Irwan, C. Bijang, and A.A. Umar, Electrocatalysis (2023) 1.
[18] M. Nurdin, O.A. Prabowo, Z. Arham, D. Wibowo, M. Maulidiyah, S.K.M. Saad, and A.A. Umar, Surfaces and Interfaces 16 (2019) 108.
[19] M. Nurdin, M. Maulidiyah, M.Z. Muzakkar, and A.A. Umar, Microchem. J. 145 (2019) 756.
[20] M. Nurdin, L. Agusu, A.A.M. Putra, M. Maulidiyah, Z. Arham, D. Wibowo, M.Z. Muzakkar, and A.A. Umar, J. Phys. Chem. Solids 131 (2019) 104.
[21] M. Nurdin, A. Zaeni, Maulidiyah, M. Natsir, A. Bampe, and D. Wibowo, Orient. J. Chem. 32 (2016) 2713.
[22] Hikmawati, A.H. Watoni, D. Wibowo, Maulidiyah, and M. Nurdin, IOP Conf. Ser. Mater. Sci. Eng. 267 (2017) 012006.
[23] Nurhidayani, M.Z. Muzakkar, Maulidiyah, D. Wibowo, and M. Nurdin, IOP Conf. Ser. Mater. Sci. Eng. 267 (2017) 012035.
[24] M. Maulidiyah, D. Wibowo, H. Herlin, M. Andarini, R. Ruslan, and M. Nurdin, Asian J. Chem. 29 (2017) 2504.
[25] I. Irwan, I.S. Jumbi, A. Alimin, R. Ratna, N. Nohong, M. Maulidiyah, M. Nurdin, and M.Z. Muzakkar, Anal. Bioanal. Electrochem. 15 (2023) 556.
[26] M. Nurdin, M. Maulidiyah, A.H. Watoni, A. Armawansa, L.O.A. Salim, Z. Arham, D. Wibowo, I. Irwan, and A.A. Umar, Korean J. Chem. Eng. 39 (2022) 209.
[27] D. Wibowo, Y. Sufandy, I. Irwan, T. Azis, M. Maulidiyah, and M. Nurdin, J. Mater.

Sci. Mater. Electron. 31 (2020) 14375.
[28] M. Śliwa, J. Podobiński, D. Rutkowska-Zbik, and J. Datka, J. Mol. Struct. 1257 (2022) 132581.
[29] P. V Bakre, D.P. Kamat, K.S. Mandrekar, S.G. Tilve, and N.N. Ghosh, Mol. Catal. 496 (2020) 111193.
[30] M. Rani, and U. Shanker, Colloids Surfaces A Physicochem. Eng. Asp. 553 (2018) 546.
[31] M. Nurdin, Z. Arham, W.O. Irna, M. Maulidiyah, K. Kurniawan, I. Irwan, and A.A. Umar, Mater. Sci. Semicond. Process. 151 (2022) 106994.
[32] Z. Arham, K. Kurniawan, and L. Anhusadar, Mater. Sci. Semicond. Process. 160 (2023) 107466.
[33] N.M. Mohamed, R. Bashiri, F.K. Chong, S. Sufian, and S. Kakooei, Int. J. Hydrogen Energy 40 (2015) 14031.
[34] M. Niu, W. Xu, S. Zhu, Y. Liang, Z. Cui, X. Yang, and A. Inoue, J. Power Sources 362 (2017) 10.
[35] J. Li, H. Yu, Z. Wu, J. Wang, S. He, J. Ji, N. Li, Y. Bao, C. Huang, and Z. Chen, Colloids Surfaces A Physicochem. Eng. Asp. 508 (2016) 117.
[36] H. Tian, S.-Z. Kang, X. Li, L. Qin, M. Ji, and J. Mu, Sol. Energy Mater. Sol. Cells 134 (2015) 309.
[37] M.P. de la Flor, R. Camarillo, F. Martinez, C. Jimenez, R. Quiles, and J. Rincon, J. Environ. Chem. Eng. 10 (2022) 107245.
[38] G. Naresh, V. Kumar, B. Sasikumar, and A. Venugopal, Appl. Catal. B Environ. 299 (2021) 120654.
[39] Z. Arham, and K. Kurniawan, Korean J. Chem. Eng. 39 (2022) 1333.
[40] Z. Arham, F.B. Awad, T. Nakai, I. Ismaun, and L. Anhusadar, Mater. Chem. Phys. 309 (2023) 128419.
[41] N. Dali, M. Maulidiyah, S. Samsiah, I. Irwan, L.O.A. Salim, Z. Arham, M. Nurdin, J. Phys. Conference Series 1763 (2021) 012067.
[42] Z. Arham, A.K. Ramli, M. Nurdin, and M. Natsir, Anal. Bioanal. Electrochem. 15 (2023) 711.
[43] M. Amatatongchai, W. Sroysee, P. Sodkrathok, N. Kesangam, S. Chairam, and P. Jarujamrus, Anal. Chim. Acta 1076 (2019) 64.
[44] X. Shi, H. Liu, M. Zhang, F. Yang, J. Li, Y. Guo, and X. Sun, Sen. Actuators B Chem. 348 (2021) 130663.